J. Electroanal. Chem., 280 (1990) 297–311
Elsevier Sequoia S.A., Lausanne – Printed in The Netherlands

Anodic dissolution of p- and n-type silicon

Kinetic study of the chemical mechanism

M.J. Eddowes

Thorn EMI Central Research Laboratories, Dawley Road, Hayes, Middlesex (Great Britain)

(Received 1 August 1989; in revised form 23 October 1989)

ABSTRACT

The anodic dissolution of silicon in fluoride containing media has been investigated experimentally. A kinetic model, consistent with the observed dissolution behaviour, is proposed. Important aspects of the reaction scheme are the involvement of the divalent intermediate silicon species and the formation of surface films on the electrode surface. The key feature of the model is its branched nature, defining the various possible reaction pathways available to certain intermediates. The reaction pathway which is operative is determined by the experimental conditions employed, important variables being the dopant type and density, the solution fluoride concentration and the applied electrode potential.

INTRODUCTION

The anodic dissolution of both p- and n-type silicon in fluoride containing media is well known. Earlier work [1,2] was concerned primarily with the electropolishing of silicon surfaces and identified conditions under which either film deposition upon, polishing of or roughening and pitting of the silicon surface occurs. Subsequently, the mechanism of the dissolution reaction was considered [3,4] in more detail and the application to selective etching according to dopant type and density was described [5–8]. More recently, there has been interest [9–13] in the photoelectrochemical dissolution of n-type silicon, in particular in the observed photocurrent doubling phenomenon. The application of electrochemical etching to the micromachining of three-dimensional structures has also been described recently [14,15].

Despite the level of both the academic and technological interest in electrochemical dissolution of silicon and the significant amount of experimental data available, no thoroughly convincing and consistent account of the reaction mechanism has been given. Two aspects fundamental to the anodic dissolution reaction can be

0022-0728/90/$03.50

identified; charge transfer from the semiconductor to intermediates at its surface and the chemistry of the dissolution of these surface intermediates. These are reflected in the dependence of the observed dissolution rate upon the silicon dopant type and concentration, the applied electrode potential and the solution conditions, in this case principally the fluoride ion concentration. In this paper, the chemical aspects of the anodic dissolution of silicon will be considered. It will be demonstrated that predictions based upon the rate equations for the proposed mechanism correlate with the observed dependence of the dissolution rate upon the relevant experimental variables. Changes in the mechanism, according to the experimental conditions employed, can be identified and are related to the surface finish obtained.

CHEMICAL MECHANISM

The early work [1] by Turner identified two types of behaviour in the anodic dissolution of silicon. Below a certain critical current density it is reported that the silicon dissolution is largely divalent and dissolution leads to deposition of a film, composed largely of silicon, on the electrode surface. Evolution of hydrogen at the anode was observed and it was suggested that this derives from the chemical oxidation by water of the divalent silicon species. Above this current density, the dissolution is largely tetravalent and gives rise to an electropolished surface. An increase in this critical current density with increase in HF concentration was established, and it was suggested that the change to electropolishing behaviour occurs when there is insufficient HF to sustain the divalent dissolution process. The formation of a thin silicon dioxide film during electropolishing was proposed, this being consistent with the conditions thought necessary [16] for electropolishing of metals.

Subsequent work [3] by Memming and Schwandt confirmed these observations. The current vs. potential curves presented by these authors show a distinct current peak which is said to correspond with the change from divalent to tetravalent dissolution. A linear Tafel plot, obtained for the current vs. potential curve in the divalent dissolution region, indicates electrochemical control of this process. In competition with the chemical oxidation of divalent silicon by water, the disproportionation reaction leading to the formation of the amorphous silicon layer on the electrode surface and a tetravalent silicon product was considered.

Later studies are generally consistent with the elements of the chemical mechanism outlined above though it has been concluded that the overall mechanism of the reaction is not well understood and that the proposed mechanism is still somewhat speculative. Undoubtedly, understanding of the mechanism is obscured by the fact that both chemical dissolution and semiconductor charge transfer processes are involved. To understand the chemical aspects fully, it will be instructive to formulate an overall reaction scheme incorporating the proposed elements of the mechanism, define the forms of the rate equations describing the various steps and then consider the implications of them as regards the reaction pathway for a given

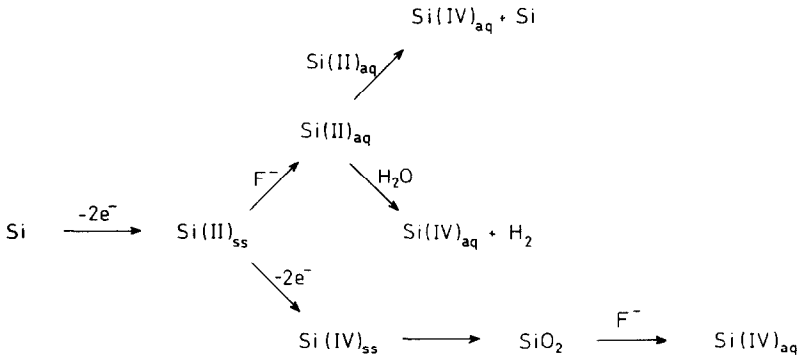

Scheme 1.

set of conditions. With the chemical aspects properly appreciated, consideration might then be given to the semiconductor charge transfer aspects of the overall process.

The basic overall reaction scheme is given in Scheme 1, in which the subscript ss denotes surface intermediate species and aq denotes those in solution. The important feature to note in this reaction scheme is its branched nature. The first stage in the process is oxidation to form $Si(II)_{ss}$, the doubly oxidised surface intermediate. This intermediate may then either undergo further oxidation to $Si(IV)_{ss}$, the fully oxidised surface intermediate, or dissolve under attack by the fluoride ligand to form the divalent solution species, $Si(II)_{aq}$. The fully oxidised surface intermediate, $Si(IV)_{ss}$, can form an oxide phase as a thin film on the silicon surface which is dissolved off by the action of fluoride to produce the fully oxidised solution species, $Si(IV)_{aq}$, presumbly the SiF_6^{2-} ion. There are two possible reaction pathways for the divalent solution species, $Si(II)_{aq}$, the one being disproportionation to form silicon and the fully oxidised solution species, $Si(IV)_{aq}$, and the other being chemical oxidation by water to form hydrogen and $Si(IV)_{aq}$.

The above mechanism is consistent with the observation of divalent and tetravalent dissolution and with the evolution of hydrogen and deposition of a silicon film during dissolution. In this respect then the proposed mechanism accounts for the reaction products. In order to establish more convincingly the validity of the proposed mechanism and to understand what determines the reaction pathway taken and product formed for a given set of conditions, we must now consider the kinetics of reaction through the relevant rate equations for the various steps.

The rate constant, $k_{e,0}$, for the first step, the surface oxidation to form $Si(II)_{ss}$, will be dependent upon the applied potential, E;

$$k_{e,0} = f_0(E) \tag{1}$$

Though there may be some additional complications associated with charge transport in the semiconductor, according to the silicon type and resistivity, for heavily doped p-type material at least, where there is a ready supply of holes, the familiar

exponential form of the rate expression for charge transfer at the surface may be expected;

$$\text{rate} = k^{\circ}_{e,0}[\text{Si}_{ss}]\{\exp(\alpha RT/nF)(E - E^{\circ})\} \quad (2)$$

The validity of this form of the rate expression is supported [3] by the reported linearity of the Tafel plot. Similarly, we may expect the rate expression for the subsequent oxidation to Si(IV)_{ss} to be potential dependent;

$$\text{rate} = k_{e,II}[\text{Si(II)}_{ss}] \quad (3a)$$

$$k_{e,II} = f_{II}(E) \quad (3b)$$

A more detailed scheme might separate the individual charge transfer steps but the simpler scheme above will be adequate for the present purposes.

The chemical dissolution steps following oxidation will be fluoride concentration dependent and independent of potential and are given by

$$\text{rate} = k_{d,II}[\text{Si(II)}_{ss}][\text{F}^-]^{n_{II}} \quad (4a)$$

$$\text{rate} = k_{d,IV}[\text{Si(IV)}_{ss}][\text{F}^-]^{n_{IV}} \quad (4b)$$

where n_{II} and n_{IV} are the number of fluoride ions involved in the rate determining steps of the dissolution of Si(II) and Si(IV) respectively. Finally, the rate of the oxidation of the divalent solution species will be given by

$$\text{rate} = k_{ox}[\text{Si(II)}_{aq}] \quad (5)$$

and the rate of its disproportionation by

$$\text{rate} = k_{disp}[\text{Si(II)}_{aq}]^2 \quad (6)$$

The important feature to note in these last two equations is that the oxidation rate will be first order with respect to the concentration of the divalent solution species and the disproportionation reaction will be second order.

Now if we consider these rate equations, in particular those at the branching points of the scheme, some understanding of the influence of the relevant experimental conditions upon the reaction pathway followed can be gained. First, as regards the two possible pathways available for the divalent surface intermediate, the dissolution process should be favoured by higher fluoride concentration and further oxidation by more positive electrode potentials, which is consistent [1–4] with earlier observations. Second, as regards the divalent solution intermediate, disproportionation should be favoured by higher concentrations of the intermediate, given the second order nature of the disproportionation reaction. To assess in more detail the validity of this chemical mechanism, further experimental work has been carried out and is presented below.

EXPERIMENTAL

Cyclic and rotating disc voltammetry and controlled potential oxidation were performed using a 1286 Electrochemical Interface (Solartron Instruments). Current

vs. potential and time profiles were recorded on a Servogor XY 743 (BBC Goerz) x–y/t recorder. Silicon samples employed were cut from wafers for standard semiconductor fabrication of ⟨100⟩ orientation, typically 0.25 to 0.3 mm thick, obtained from Wacker Chemitronic GmbH. Electrical contact to these was made via an indium solder back contact and they were mounted in a PTFE rotating disc electrode system constructed in this laboratory, leaving an exposed electrode area of 71 mm^2 (a 9.5 mm diameter disc). In some cases photolithographically patterned squares with an exposed electrode area of 10 mm^2 were employed. Photo-electrochemical experiments were performed in a PTFE cell with a sapphire window in the base to allow illumination of n-type material. The counter electrode was a large platinum gauze cylinder. In some experiments the reference electrode employed was a saturated calomel electrode, held separately from the main cell and connected via a PTFE capillary tube. However, it was found that contamination of the etchant solution with KCl could significantly alter film formation on the silicon electrode surface and hence affect the observed dissolution behaviour. Consequently, it was found more convenient to employ a silver wire reference for many experiments. For most of the photoelectrochemical studies the light source was a quartz–halogen lamp from a conventional slide projector. In some cases an 8 mW helium–neon laser (Uniphase) with beam expanding optics was employed. All experiments were carried out in an unlit fume cupboard under relatively low ambient light conditions but without any rigorous attempt to exclude ambient light. Any direct photocurrent effects under these ambient lighting conditions were negligible compared with the reported anodic dissolution currents.

In most experiments the electrolyte solution employed was a standard silicon dioxide etchant solution (Chemwell International) composed of a 13 : 2 mixture of 40% ammonium fluoride and 48% hydrofluoric acid. This was diluted as required using doubly distilled, de-ionised water. Hydrofluoric acid was obtained from BDH Limited.

RESULTS

Anodic dissolution of p-type silicon

A typical current vs. potential curve obtained for heavily doped p-type silicon (0.075–0.125 Ω cm) in $HF + NH_4F$ oxide etchant solution is shown in Fig. 1. This shows two distinct current peaks, in contrast to the single peak reported [3,4] in earlier studies. At potentials positive of the second current peak the current reaches a steady value and then increases further with increasing potential beyond +5 V. The same curve is followed in both forward and reverse potential sweeps, at lower scan rates at least, and is fairly insensitive to the rate of solution stirring. From this it may be concluded that the current vs. potential curves obtained represent the steady state behaviour, limited by the rate of the surface reaction rather than transport of reactants and products, and that the peaks are associated with film formation upon the electrode surface. The magnitude of the observed current peaks varies with fluoride concentration, as shown in Fig. 1. The magnitude of the first

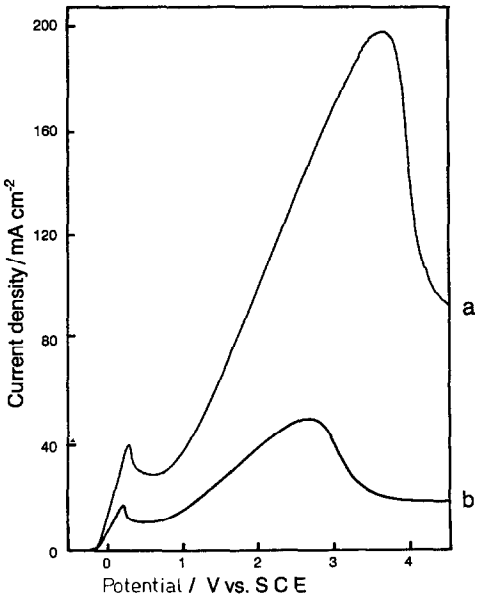

Fig. 1. Current vs. potential curves obtained for p-type silicon (0.075–0.125 Ω cm) in standard oxide etchant at a dilution of (a) 0.1; (b) 0.05.

peak is found to vary linearly with fluoride concentration and that of the second peak linearly with the square of the fluoride concentration, as illustrated in Fig. 2.

At potentials below that of the first current peak, gas is evolved at the anode and this gas evolution ceases once the potential of the first current peak is reached. It is assumed that this is hydrogen evolution, due to chemical oxidation of divalent silicon solution species, as outlined above in the discussion of the reaction scheme and reported [1,2] in earlier studies. At potentials within a few hundred millivolts of the potential of onset of dissolution, the current obeys the Tafel equation, as illustrated in Fig. 3, from which it is concluded that the rate expression has the form given in eqn. (2). A slope of 106 mV decade^{-1}, translating to a value for $\alpha nF/RT$ of 21.7 and hence a value for αn of approximately $\frac{1}{2}$, is obtained from this Tafel plot.

A further point of interest is the variation of the dissolution valence as a function of the applied potential. This was measured by means of coulometry and determination of sample weight loss following controlled potential oxidation. The results, given in Fig. 4, show that below the potential of the first current peak the dissolution valence is close to 2. Above this potential an increase in the dissolution valence is observed, rising steadily towards 4 as the potential increases towards that of the second peak. This behaviour is generally consistent with that observed previously [3,4] but the switch from a dissolution valence of 2 to one of 4 is not as abrupt as indicated [3] by Memming and Schwandt.

Silicon samples of higher resistivity also were found to exhibit current vs. potential curves with two current peaks, of essentially the same magnitude as those

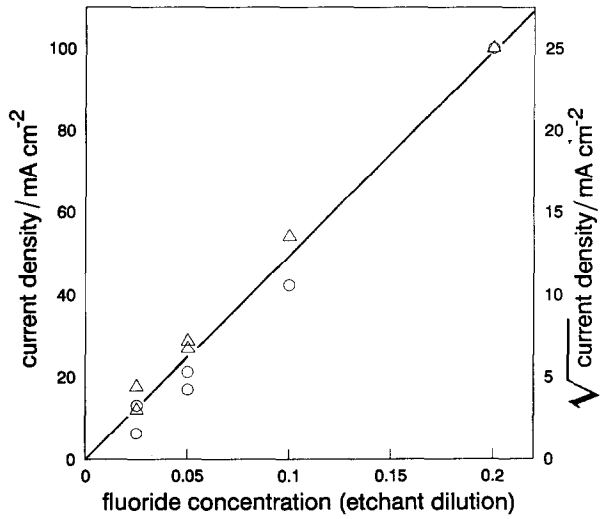

Fig. 2. Variation of: (○), first current peak height; (△), square root of second current peak height with fluoride concentration in etchant solution.

observed for the heavily doped samples. However, these are spread out to more positive potentials, as illustrated in Fig. 5 and this behaviour is generally consistent with that reported previously.

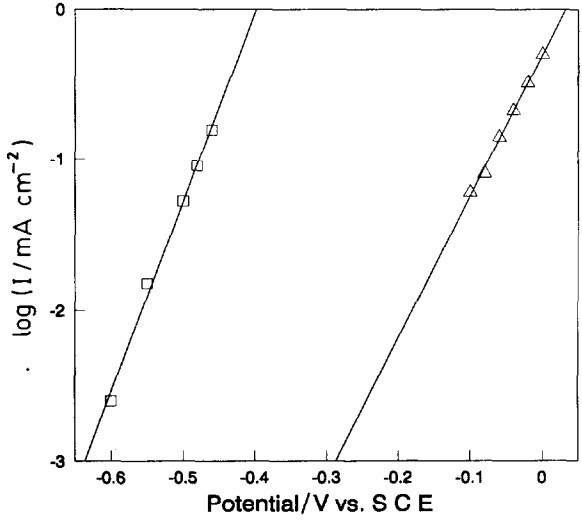

Fig. 3. Tafel plot for anodic dissolution in fluoride etchant of (△) p-type silicon (0.075–0.125 Ω cm); (□) n-type silicon (14–20 Ω cm). The light intensity employed for the n-type oxidation was sufficient to give an illumination intensity limited current of 2.7 mA cm^{-2} at potentials greater than −0.3 V vs. SCE.

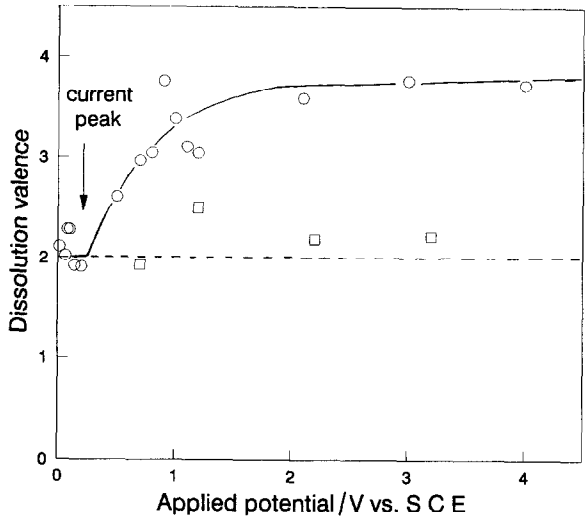

Fig. 4. Dissolution valence for controlled potential oxidation of (○) p-type silicon (0.075–0.125 Ω cm); (□) n-type silicon (0.375–0.625 Ω cm) under illumination intensity limitation, against applied potential of oxidation.

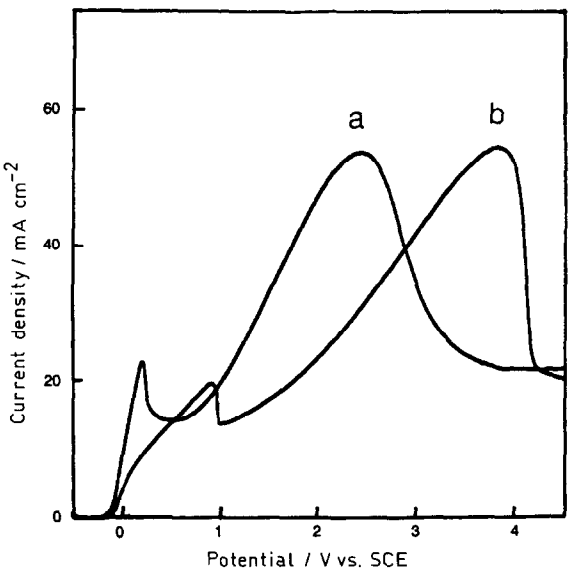

Fig. 5. Current vs. potential curve obtained for (a) p-type silicon (0.075–0.125 Ω cm), (b) p-type silicon (4–6 Ω cm) in oxide etchant at a dilution of 0.05.

A point of practical importance which might also shed light on the kinetics of the dissolution process is the nature of the surface finish obtained following controlled potential oxidation. At potentials positive of the first current peak a smooth electropolished surface is obtained. No further assessment of the variation in quality of this electropolished finish with applied potential beyond the first current peak has been carried out. At potentials less positive than the first current peak, according to the exact conditions employed, a rough pitted surface may develop or a brown deposit may form on the electrode surface, as reported [1–4] earlier. This deposit, which has been characterised [1,2] as containing primarily silicon and is considered to be formed by the disproportionation reaction of the $Si(II)_{aq}$ solution species, may be either smooth and amorphous or may exhibit crystalline features. The factors determining the exact nature of the surface finish obtained at potentials less positive than the first current peak have not been investigated further and would warrant attention.

Anodic dissolution of n-type silicon

The behaviour of n-type silicon samples with resistivities of 0.375–0.625, 4–6 and 14–20 Ω cm has been investigated. In the absence of light, practically no oxidation current is observed at anodic polarisations up to +10 V. Under illumination of sufficient intensity, a current vs. potential curve with two current peaks, similar to that obtained with p-type silicon, is observed, as illustrated in Fig. 6. The peak height vs. fluoride concentration relationship for n-type silicon is found to be consistent with that for p-type silicon, illustrated in Fig. 2. At lower illumination intensities an intensity limited current plateau is observed and under these condi-

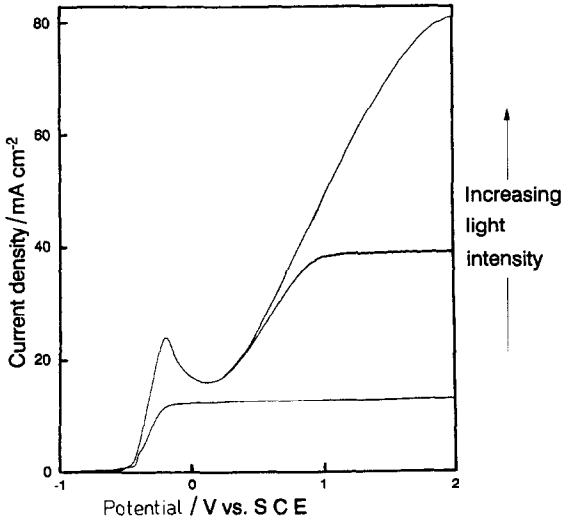

Fig. 6. Current vs. potential curve obtained for n-type silicon (14–20 Ω cm) in oxide etchant at a dilution of 0.05 at a range of illumination intensities.

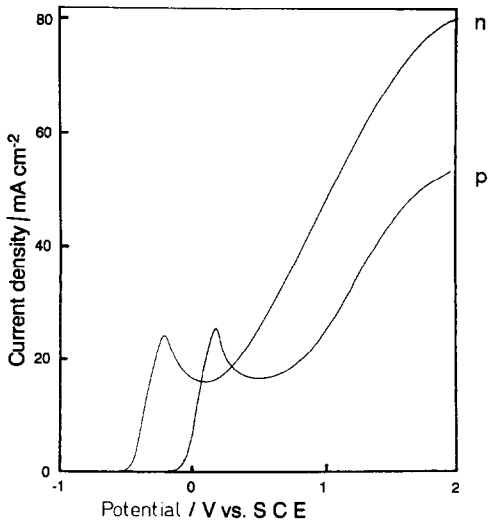

Fig. 7. Comparison of current vs. potential curves for p-type (0.075–0.125 Ω cm) and n-type (14–20 Ω cm) silicon.

tions it appears that the dissolution rate is determined by the supply of photo-generated holes rather than the rates of surface electron transfer or chemical dissolution processes.

Compared with the current vs. voltage curve for p-type material, that for n-type silicon under illumination is displaced to more negative potentials, as illustrated in Fig. 7. This displacement is consistent with the higher potential of the Fermi level relative to the valence band edge in n-type silicon than in p-type silicon, leading to a lowering in the applied potential at which the bands are appropriately bent at the surface to allow hole transport to the surface. The Tafel plot for n-type silicon, shown in Fig. 3, is linear with a slope of 80 mV, translating to a value for $\alpha nF/RT$ of 27.6 and hence a value for αn of approximately 0.7.

As for the p-type material, the dissolution valence was determined for n-type silicon. At higher illumination intensities, where the process is not light intensity limited and the current vs. voltage curve obtained has essentially the same form as that of the p-type silicon with two current peaks, the dissolution valence determined fits that obtained for p-type material with a value of 2 below the first current peak increasing from 3 to 4 with increasing potential above the first current peak. For the light intensity limited etch, where the dissolution current reaches its limiting value at a potential below that of the first current peak, the value for the dissolution valence was found to be close to 2 even at higher oxidation potentials, as illustrated in Fig. 4.

The surface finishes obtained for n-type silicon are also similar to those obtained for p-type material, electropolished surfaces being produced at potentials above the first current peak and rough surfaces resulting from oxidation at potentials below

this and at lower illumination intensities where the light intensity limited current is below that of the first current peak.

DISCUSSION

Having proposed a kinetic scheme, as shown in Scheme 1, and determined the kinetic characteristics of silicon dissolution in terms of current vs. voltage curves, we may now assess the correlation between the model and observed behaviour. The experimental results obtained in this study differ from those previously reported in the observation of two rather than a single current peak in the current vs. potential curves. The occurrence of these two current peaks and the gradual change of the dissolution valence between values of 3 and 4 at potentials positive of the first current peak would appear to indicate some inadequacy in the proposed reaction scheme. However, a proper interpretation of the basic model can explain the nature of the observed current vs. voltage curves as follows.

At potentials below the first current peak the dissolution process is essentially divalent and, as indicated by the linearity of the Tafel plot, is an electrochemical rate controlled process. The observation of silicon deposition and hydrogen evolution is consistent with the disproportionation and chemical oxidation reactions given in the reaction scheme. The balance between the degree to which the one or other process occurs will presumably depend on the detail of the experimental conditions employed. With the disproportionation process second order with respect to the divalent solution species, $Si(II)_{aq}$, and the chemical oxidation first order, as given by eqns. (4a) and (4b), the disproportionation reaction would be favoured at higher current densities which generate high concentrations close to the electrode surface. Conversely, chemical oxidation will be favoured by low current densities and the corresponding low concentrations close to the electrode surface. This may explain the differences in the exact nature of the finish obtained following oxidation at potentials below the first current peak. However, no systematic study of this aspect has been carried out as yet.

The involvement of a divalent solution species might appear at first sight a little surprising. However, there is no reason to suppose that the divalent surface state should necessarily be any more chemically stable than the solution species. In fact, the considerable strength of the silicon–fluorine bond, as compared with the silicon–silicon bond, might be considered to favour the dissolution by fluoride. The competition between dissolution and further oxidation must depend on the relative magnitudes of the rate constants for the two reactions and it would appear that, under these circumstances at least, dissolution by fluoride is the faster process. It may be concluded that the portion of the proposed reaction scheme involving dissolution of the divalent surface state and the reactions of the divalent solution species accounts adequately for the experimentally observed behaviour.

For the proposed scheme, as the applied potential increases the rate of formation of oxidised surface species increases, in accordance with the rate expression given in eqn. (2). As this rate increases, oxidised surface species may eventually be produced

faster than the rate at which they can be dissolved by the available fluoride, according to eqn. (4a), and will then form a layer on the electrode surface. The overall dissolution rate will then be controlled by the dissolution step rather than the oxidation step and the current may drop as the potential increases, given that the layer is chemically distinct from the oxidised surface state and dissolves at a slower rate. Under these circumstances, a peak in the current vs. potential curve is to be expected corresponding with the maximum rate for dissolution of the oxidised surface state by fluoride. This rate will be dependent upon fluoride concentration and hence the peak current will be fluoride concentration dependent, as illustrated in Fig. 2. The model therefore predicts a peak in the current vs. potential curve and formation of a layer on the electrode surface irrespective of the valence of the oxidation process at the potential of the current peak. It is not necessary that the current peak be correlated with the switch from a dissolution valence from 2 to 4, as suggested [2] in earlier work. All that is required is that the rate of formation of the oxidised intermediate surface state, whatever its oxidation state, exceeds that of its dissolution. The observed current vs. potential behaviour (Fig. 1) is entirely consistent with this mechanism, the oxidised surface state dissolution process being first order in fluoride (Fig. 2) and the surface layer probably being an oxide or mixed oxide/fluoride of silicon with a formal valence of approximately 3. The onset of electropolishing at the potential of the first current peak is consistent with the surface layer formation.

The second order dependence upon fluoride concentration of the observed rate at potentials positive of the first current peak, as illustrated in Fig. 2, demonstrates the involvement of fluoride in the reaction mechanism over this potential range. Dissolution of the surface layer would appear to be the probable chemical rate determining process involved. Once this layer has formed upon the electrode surface the overall dissolution process will consist of three steps; electron transfer at the silicon/surface layer interface, counter ion migration across the surface layer to this interface and dissolution by fluoride of the surface layer at its interface with the electrolyte. With the rate determining step being a chemical process one might expect the rate to be potential independent, though this is clearly not observed experimentally. However, as the potential increases and the rate, given by eqn. (3), of the subsequent electron transfer reaction increases, demonstrated by the change in the dissolution valence, a corresponding increase in the dissolution current is to be expected. The increase in current with potential exceeds that expected purely on the basis of the increase in dissolution valence. However, as the dissolution valence changes, the chemical nature of the film will also change, along with its rate of dissolution by fluoride. An increase in the current with potential is therefore not inconsistent with the chemical dissolution of the surface layer being the rate determining step. At potentials beyond the second current peak the plateau in the current, as shown in Fig. 1, is consistent with chemical rather than electrochemical rate control and indicates that the chemical nature of the film changes little over this potential range.

To account fully for the two current peaks rather than the single peak reported

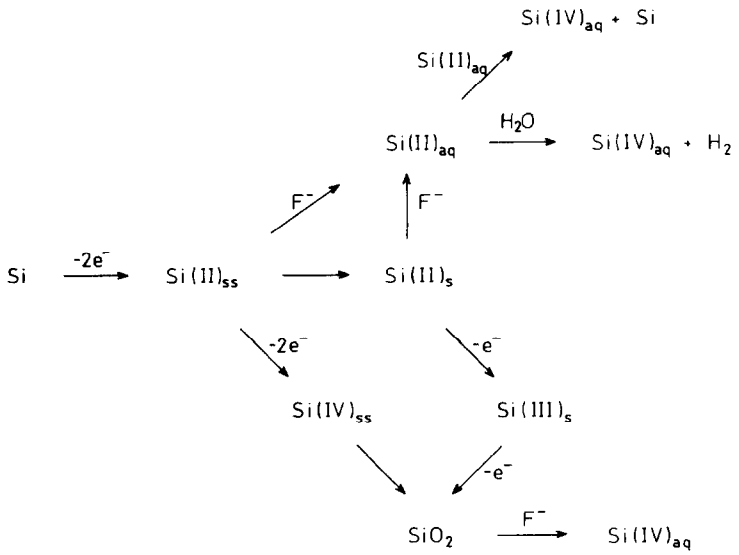

Scheme 2.

earlier, some modification to the proposed reaction scheme is required: a single branching point in the mechanism at the divalent surface state is not sufficient. This will include solid phase silicon species formally divalent and trivalent as well as tetravalent. This is shown in Scheme 2, where $Si(II)_s$, $Si(III)_s$ and SiO_2 represent the types of solid phase intermediates in the surface layer. Clearly, there are a wide variety of possible mixed valence intermediates which might occur in the surface film, giving this film a formal valence between 2 and 4. To identify the chemical nature of these intermediates, spectroscopic studies of the type demonstrated recently [13] may be helpful: kinetic studies of the type described here cannot be expected, alone, to provide much more than an indication of the possible types of intermediates that might be involved.

In addition to the chemical aspects of the process, the model must account for semiconductor charge transport aspects, though this has not been a primary concern of the work presented here. In general it may be said that the anodic dissolution of silicon samples of different donor type and density exhibit the same general chemical characteristics. That is to say they all show a current vs. potential curve with two distinct peaks, of essentially the same magnitude for any silicon sample for a given set of solution conditions, consistent with the concept of the critical current density described in earlier studies. Gas evolution is observed at potentials below the first current peak and electropolishing at potentials above it: the dissolution valence is essentially 2 at potentials below the first current peak and rises from around 3 to 4 as the potential is increased above it. The difference between the dissolution behaviour of n- and p-type silicon is simply the requirement of the former for illumination and the direct oxidation of the latter. As discussed in earlier

studies, this can be related to the requirement for holes during the oxidation, these being present inherently in p-type material and inherently absent but generated by illumination in n-type material. From this it appears that samples of different resistivity exhibit essentially the same dissolution chemistry. Spreading of the potential axis in the current vs. voltage curves may be due to a combination of a variation in interfacial electron transfer rates with sample resistivity and voltage drops as a result of the current flow across the silicon sample causing the surface potential to be lower than that applied to the back of the sample.

The spreading of the current vs. potential curve along the potential axis with increasing resistivity of p-type silicon samples indicates an increasing limitation on charge transfer with reduction in dopant concentration. This may be associated both with voltage drops across the bulk of the semiconductor due to its resistance and differences in the interfacial space charge layer and its charge transfer characteristics. It is concluded that, for a given rate of charge transport to the surface and hence rate of surface oxidation, the chemical aspects of the dissolution will be essentially the same for all silicon samples. What will vary between samples is the potential and illumination conditions required to achieve that given rate of charge transport.

CONCLUSIONS

In summary, the general chemical kinetic model proposed can account for the nature of the observed current vs. potential behaviour of the anodic dissolution of silicon. The important characteristic of the proposed reaction scheme is its branched nature and the dependence of the rates of the different available pathways on different chemical and electrochemical variables. These variables determine which pathway is taken under a given set of conditions. There remains considerably more detail of the reaction mechanism to be elucidated, in particular relating to the chemical nature of the layers formed on the electrode surface and the interfacial charge transfer processes involved in the oxidation step.

ACKNOWLEDGEMENTS

The author wishes to thank Miss E. Lueng who performed a substantial part of the experimental work reported above.

REFERENCES

1 D.R. Turner, J. Electrochem. Soc., 103 (1958) 402.
2 D. Baker and J.R. Tillman, Solid State Electron., 6 (1963) 589.
3 R. Memming and G. Schwandt, Surf. Sci., 4 (1966) 109.
4 R.L. Meek, J. Electrochem. Soc., 118 (1971) 437.
5 H. van Dijk and J. de Jonge, J. Electrochem. Soc., 117 (1970) 553.
6 M.J.J. Theunissen, J.A. Appels and W.H.C.G. Verkuylen, J. Electrochem. Soc., 117 (1970) 959.
7 M.J.J. Theunissen, J. Electrochem. Soc., 118 (1971) 351.

8 R.L. Meek, J. Electrochem. Soc., 118 (1971) 1240.
9 M. Matsumura and S.R. Morrison, J. Electroanal. Chem., 144 (1983) 113.
10 M. Matsumura and S.R. Morrison, J. Electroanal. Chem., 147 (1983) 157.
11 H. Gerischer and M. Lubke, Ber. Bunsenges. Phys. Chem., 91 (1987) 394.
12 H. Gerischer and M. Lubke, J. Electrochem. Soc., 135 (1988) 2782.
13 L.M. Peter, D.J. Blackwood and S. Pons, Phys. Rev. Lett., 62 (1989) 308.
14 L. Tenerz, Electron. Lett., 21 (1985) 1207.
15 Z. Shengliang, Z. Zongmin and L. Enke, Proceedings of Transducers '87, The Fourth International Conference on Solid-State Sensors and Actuators, Tokyo, Institute of Electrical Engineers of Japan, Tokyo, 1987, p. 130.
16 D. Landolt, Electrochim. Acta, 32 (1987) 1.